



# Palladium nanocrystals stabilized by cucurbit[6]uril as efficient heterogeneous catalyst for direct C–H functionalization of polyfluoroarenes



Minna Cao, Dongshuang Wu, Weiping Su, Rong Cao<sup>\*</sup>

State Key Laboratory of Structural Chemistry, Fujian Institute of Research on the Structure of Matter, The Chinese Academy of Science, Fuzhou 350002, China

## ARTICLE INFO

### Article history:

Received 6 August 2014

Revised 23 October 2014

Accepted 25 October 2014

### Keywords:

C–H functionalization

Palladium

Nanocrystals

Cucurbit[6]uril

Heterogeneous

## ABSTRACT

Palladium nanocrystals (Pd NCs) featuring abundant surface defects are successfully synthesized by using cucurbit[6]uril as a stabilizer. Employing the as-prepared Pd NCs as catalyst, an efficient approach to the direct C–H functionalization of electron-deficient polyfluoroarenes has been developed. The stable Pd NCs catalyst exhibits excellent catalytic activity and good recyclability with significantly low catalyst loading. The catalytic procedure is insensitive to air and moisture and can be manipulated under ambient environment with operational ease. Mechanistic experiments have provided credible data to support a heterogeneous catalytic mechanism of the present system.

© 2014 Elsevier Inc. All rights reserved.

## 1. Introduction

In the recent years, the direct arylation via C–H bond activation to afford the corresponding biaryl structural motif has become the focus of synthetic chemists. Compared to traditional methods, the approach to direct arylation can avoid the preparation of aryl organometallics with higher atom and step efficiency [1–4]. In this regard, huge progress has been achieved with homogeneous catalysis [5–8]. Homogeneous catalysis is generally accepted because it is easily to tune the chemo-, regio-, and enantioselectivity of the catalyst. However, the high catalyst loading, using expensive and not easily to synthesized ligands, strictly required reaction conditions (e.g., sensitive to moisture and water), and the difficulty of catalyst separation from product created economic and environmental obstacles to broaden their scope and commercialization. Additionally, many direct arylation reactions require utilization of unstable, toxic, and expensive phosphine ligands, whose price is even beyond that of noble metal. When taking the high cost of the whole procedure of homogeneous catalysis and the improvement of the transformation efficiency into consideration, however, it is still highly desirable to develop new catalysis systems featured recycling, continuous processing, and ease of separation to offer green and cost-effective alternatives for C–H functionalization.

Metal nanocrystals (NCs) have shown excellent catalytic activities toward electrochemical catalysis, photocatalysis, and organic synthesis because of their high-surface-to-volume ratio and quantum size effects. In the past decades, researchers have made significant advances in the synthesis of well-defined NCs for organic syntheses by modifications of preparation conditions, support materials, and capping agents [9–17]. For instance, there is a long history of synthesizing size-controlled noble metal NCs by cyclodextrins through their ability to form inclusion complexes or supramolecular adducts with organic molecules or metal precursors. These metal NCs are active for hydrogenation reactions carried out in aqueous or gas-phase media [18–20]. To date, great achievements have been made in gas–liquid reactions such as hydrogenation of nitroaromatics, as well as some simple liquid-phase reactions with low activation energy such as Suzuki coupling reaction [21–25]. Nevertheless, many organic syntheses in liquid phase, for example, the direct arylation of electron-deficient polyfluoroarenes through C–H bond activation, have not been succeed on metal NCs to date. The high activation energy for C–H bond activation of this reaction puts forward much higher demands for the NCs, that is, abundant active sites on the metal NCs and good enough reusability [26,27]. Given the practical application for industries, effective catalytic system using nanostructured catalysts with simple catalytic procedure and good reusability but without sacrificing catalytic activity still presents significant and formidable challenges for organic synthesis, especially for those that are only accessible in homogeneous catalysis.

<sup>\*</sup> Corresponding author. Fax: +86 0591 83796710.

E-mail address: [rcao@fjirsm.ac.cn](mailto:rcao@fjirsm.ac.cn) (R. Cao).

In this work, by using cucurbit[6]uril (CB[6]) stabilized palladium NCs as catalyst, we report an efficient approach to the direct arylation of polyfluoroarenes with aryl halides to construct biaryls. The well-defined Pd NCs are characteristic of abundant surface defects, and thus endows the Pd NCs with excellent catalytic activity. Due to the stabilization from cucurbit[6]uril, the surface defects of Pd NCs have remained after catalysis. The stable Pd NCs catalyst exhibits excellent catalytic activity and good recyclability with significantly low catalyst loading. Additionally, through this method, the catalytic reaction can be carried out under air conditions with operationally simple procedures using significantly low catalyst loadings, which exhibits a great potential in reducing the overall cost of practical applications and is important to pharmaceutical and green chemistry. In addition, we have carried out mechanistic experiments to support a heterogeneous mechanism of the present system in this work.

## 2. Experimental

### 2.1. Materials

Cucurbit[*n*]uril was prepared according to literatures [28]. All other reagents were commercial available and used as received without further purification.

### 2.2. Instruments and characterization

X-ray diffraction patterns (XRD) were recorded with a Rigaku D/max-2500 X-ray powder diffractometer with Cu K $\alpha$  radiation ( $\lambda = 0.154$  nm). TEM and HR-TEM images were recorded by a FEI Tecnai G2 F20 working at 200 kV. The samples were prepared by placing a drop of product in water onto a continuous carbon-coated copper TEM grid. Analysis of Pd content was measured by inductively coupled plasma-atomic emission spectroscopy (ICP-AES) on an Ultima 2 analyzer (Jobin Yvon). The gas chromatography–mass spectrometry (GC–MS) measurements were taken on a Varian 450-GC/240-MS.  $^1\text{H}$  NMR (400 MHz), and  $^{13}\text{C}$  NMR (100 MHz) spectra were recorded in CDCl $_3$  solutions using a Bruker Avance 400 spectrometer.

### 2.3. Catalyst preparation

CB[6] (stabilizer, 398 mg, 0.40 mmol) and PdCl $_2$  (metal precursor, 35 mg, 0.20 mmol) were mixed in distilled water (40 mL) and stirred for overnight to obtain a uniform brown mixture. Then, the mixture was adjusted to pH 1 by using 6 M hydrochloric acid aqueous solution. The mixture was turned into black immediately after NaBH $_4$  aqueous solution (76 mg in 20 mL water) was injected quickly. The final product (denoted as CB[6]–Pd NCs) was separated from solution by centrifugation after 3 h, washed twice with water, and dried in an oven overnight.

For comparison, Pd NCs stabilized by other three common cucurbit[*n*]uril have been prepared by the same reducing method with CB[6]–Pd NCs, and the final products were denoted as CB[*n*]–Pd NCs (*n* = 5, 7, 8).

### 2.4. General catalytic procedure and analyzes

A mixture of pentafluorobenzene (1.5 mmol, 1.5 equiv.), aryl halides (1.0 mmol, 1.0 equiv.), sodium carbonate (2 mmol, 2 equiv.), acetic acid (2 mmol, 2 equiv.) and the as-prepared Pd NCs catalyst (1 mol%) was added into a 35 mL pressure tube. Then, 2 mL mixed solvent solution of DMA/DMF (0.6/1.4) was added. The reaction mixture was stirred at 140 °C for 24 h under ambient atmosphere. After the reaction was completed, the solid catalyst

was separated by filtration, and the filtrate was diluted with water followed by extraction with ethyl acetate (3  $\times$  10 mL), and dried over anhydrous Na $_2$ SO $_4$ . The solvent was removed by vacuum rotary evaporation, and the crude product was directly analyzed by GC–MS with *n*-dodecane as an internal standard. The product was further purified by column chromatography (silica gel, ethyl acetate/hexane gradient) for NMR.

Catalyst recycling experiments: Five recycles of the activity were examined for the as-prepared Pd NCs catalyst. After the 1st run, the catalyst was separated by centrifugation and then washed with ethyl acetate (EtOAc) and water to remove adsorbed organic substrate and salt, followed by drying overnight at 70 °C prior to being reused. The catalyst was used for the 2nd run without further activation, and the same process was repeated for the next run.

Applications of hot filtration: Hot filtration was carried out after 2 h for the direct arylation of pentafluorobenzene with bromobenzene. The filtrates were further reacted under the same conditions for another 20 h after fresh base and additive added. The yields were analyzed by GC–MS with *n*-dodecane as an internal standard.

Mercury drop test: A model reaction was added a drop of Hg(0) after 8 h and then reacted under the same conditions for another 16 h. The yields were analyzed by GC–MS with *n*-dodecane as an internal standard.

## 3. Results and discussion

### 3.1. Synthesis of Pd NCs catalyst

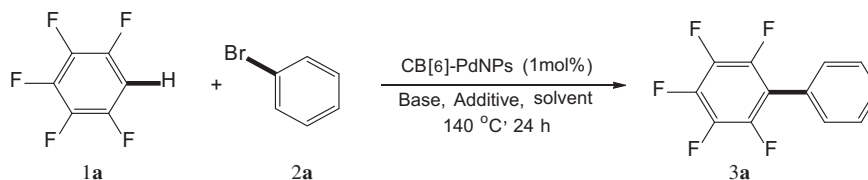
Pd NCs catalyst was prepared by reducing metal precursor in the presence of cucurbit[6]uril. CB[6] is a hexameric macrocyclic compound comprising six glycoluril units and twelve methylene bridges. It belongs to a family of macrocyclic organic compounds, cucurbit[*n*]uril (CB[*n*], *n* = 5–8), which are prepared by an acid-catalyzed condensation reaction. The CB[6] molecules here are stabilizer, which are capable of binding to other species through electrostatic interaction, helping stabilize the Pd NCs from agglomeration. Due to the high surface energies, nanostructures generally tend to aggregate, leading to the loss of the fascinating properties for longtime storage and applications. Herein, the steric effect arising from the rigid cyclic structure of CB[6] can prevent the Pd NCs from aggregation effectively. Therefore, the Pd NCs stabilized by CB[6] sustain excellent catalytic performance without reactivation even after longtime storage in air [29–33].

### 3.2. Catalytic performance of the as-prepared Pd NCs

The catalytic activity of the as-prepared Pd NCs was examined by the direct arylation of pentafluorobenzene (1a) with bromobenzene (2a) as the model reaction. Selected results from the reaction conditions optimization studies are listed in Table 1. Preliminary results indicate that bases, solvents, and additives appear to be key factors affecting the catalytic efficiency of the as-prepared Pd NCs. The desired product was obtained in 39% yield if the reaction was performed with Na $_2$ CO $_3$  (2 equiv) as base in DMF (N,N'-dimethylacetamide) (2 mL) (Table 1, Entry 4). Using acetic acid (2 equiv.) as additive affords a satisfied yield up to 82% (Table 1, Entry 10). Subsequently, the influence of solvent on the reaction was investigated (Table 1, Entries 12–17). Solvent screening gave a maximum yield of 96% in a mixed solution of DMA/DMF under the reaction conditions detailed in Table 1 (Table 1, Entry 17). Under such conditions, a remarkable 99% yield of the cross-coupled direct arylation product can be achieved if the reaction is allowed to proceed for a longer time to 26 h (Entry 18 in Table 1). In addition, the effect of the catalyst loading was examined (Table 1, Entries 19–22). If the amount of catalyst was reduced to 0.05 mol%,

**Table 1**

Selected results from the optimization studies for CB[6]-Pd NPs catalyzed direct arylation of pentafluorobenzene with bromobenzene[a].



Entry	Base	Additive <sup>[b]</sup>	Solvent <sup>[c]</sup>	Yields (%)
1	NaOAc	-	DMA	16
2	KOAc	-	DMA	26
3	CsOAc	-	DMA	trace
4	Na <sub>2</sub> CO <sub>3</sub>	-	DMA	39
5	K <sub>2</sub> CO <sub>3</sub>	-	DMA	11
6	Cs <sub>2</sub> CO <sub>3</sub>	-	DMA	trace
7	NaOPiv	-	DMA	0
8	Na <sub>2</sub> CO <sub>3</sub>	HCOOH	DMA	0
9	Na <sub>2</sub> CO <sub>3</sub>	PivOH	DMA	0
10	Na <sub>2</sub> CO <sub>3</sub>	AcOH	DMA	82
11	K <sub>2</sub> CO <sub>3</sub>	AcOH	DMA	24
12	Na <sub>2</sub> CO <sub>3</sub>	AcOH	DMSO	0
13	Na <sub>2</sub> CO <sub>3</sub>	AcOH	NMP	35
14	Na <sub>2</sub> CO <sub>3</sub>	AcOH	Toluene	0
15	Na <sub>2</sub> CO <sub>3</sub>	AcOH	DMF	27
16	Na <sub>2</sub> CO <sub>3</sub>	AcOH	DMA/DMF (1/1)	60
17	Na <sub>2</sub> CO <sub>3</sub>	AcOH	DMA/DMF (0.6/1.4)	96 (93)
18 <sup>[c]</sup>	Na <sub>2</sub> CO <sub>3</sub>	AcOH	DMA/DMF (0.6/1.4)	99
19 <sup>[d]</sup>	Na <sub>2</sub> CO <sub>3</sub>	AcOH	DMA/DMF (0.6/1.4)	88
20 <sup>[e]</sup>	Na <sub>2</sub> CO <sub>3</sub>	AcOH	DMA/DMF (0.6/1.4)	76
21 <sup>[f]</sup>	Na <sub>2</sub> CO <sub>3</sub>	AcOH	DMA/DMF (0.6/1.4)	78
22 <sup>[g]</sup>	Na <sub>2</sub> CO <sub>3</sub>	AcOH	DMA/DMF (0.6/1.4)	68
23 <sup>[h]</sup>	-	AcOH	DMA/DMF (0.6/1.4)	0
24 <sup>[h]</sup>	Na <sub>2</sub> CO <sub>3</sub>	AcOH	DMA/DMF (0.6/1.4)	0
25 <sup>[i]</sup>	Na <sub>2</sub> CO <sub>3</sub>	AcOH	DMA/DMF (0.6/1.4)	30
26 <sup>[j]</sup>	Na <sub>2</sub> CO <sub>3</sub>	AcOH	DMA/DMF (0.6/1.4)	66
27 <sup>[k]</sup>	Na <sub>2</sub> CO <sub>3</sub>	AcOH	DMA/DMF (0.6/1.4)	65

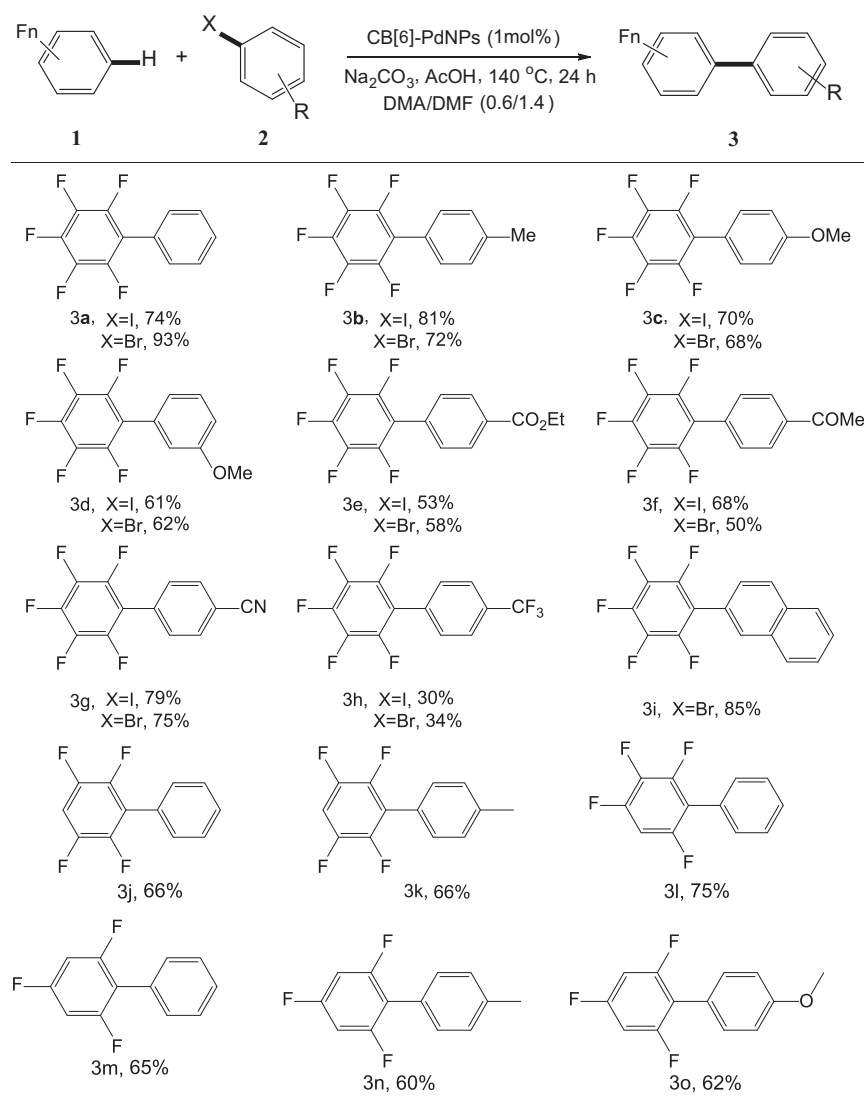
[a] Reaction conditions: The reactions were carried out in the air using pentafluorobenzene (1.5 equiv.), bromobenzene (1 equiv.), base (2 equiv.), additive (2 equiv.), and 1 mol% catalyst, in a 0.5 M solvent solution for 24 h under 140 °C, unless otherwise noted. [b] Determined by GC analysis relative to as an internal standard (isolated yield in parentheses). [c] 26 h. [d] 0.5 mol% catalyst loading. [e] 0.25 mol% catalyst loading. [f] 0.1 mol% catalyst loading. [g] 0.05 mol% catalyst loading. [h] Without CB[6]-Pd NPs catalyst. [i] 1 mol% CB[5]-Pd NPs catalyst loading. [j] 1 mol% CB[7]-Pd NPs catalyst loading. and [k] 1 mol% CB[8]-Pd NPs catalyst loading.

the yield only decreased to 68% (Table 1, Entry 22). The decrease in the catalyst loading also afforded such good yield of the required product, indicating that the as-prepared Pd NCs is a highly active catalyst for the direct arylation of pentafluorobenzene. Control experiments demonstrated that no reaction was observed in the absence of the Pd NCs with or without Na<sub>2</sub>CO<sub>3</sub>/AcOH (Entries 23 and 24 in Table 1), suggesting that the as-prepared Pd NCs actually act as the real catalyst. Finally, we found that satisfied result was

obtained by reacting a ratio of 1a and 2a of 1.5:1, using 2 equiv. of Na<sub>2</sub>CO<sub>3</sub> as base in conjunction with 2 equiv. AcOH as additive in a mixed solution of DMA and DMF (0.6/1.4) with 1 mol% of the as-prepared Pd NPs catalyst in 24 h at 140 °C in air (Entry 17, Table 1). Remarkably, the catalytic reaction is operationally simple and insensitive to air and moisture.

Using the same preparation procedure, we also prepared Pd NCs in the presence of CB[5], CB[7], and CB[8]. These three CB[n] (n = 5,

**Table 2**  
The Pd NCs catalyzed direct arylation of fluoroarenes with various aryl halides.[a]



[a] Reaction conditions: The reactions were carried out in the air using fluoroarenes (1.5 equiv.), aryl halides (1 equiv.),  $\text{Na}_2\text{CO}_3$  (2 equiv.), AcOH (2 equiv.), solvent: DMA/DMF (0.6/1.4), and 1 mol% Pd NCs catalyst, in a 0.5 M solvent solution for 24 h under 140 °C; Isolated yields unless otherwise noted.

7, 8) have the similar structural features but different physical and chemical properties to give them distinct behaviors and appearances as Pd nanoparticles catalyst stabilizer. The TEM and high-resolution (HR) TEM images for CB[n]-Pd NCs ( $n = 5, 7, 8$ ) illustrate that these three Pd NCs are uniformly dispersed but with different morphologies as compared with Pd NCs stabilized by CB[6] (Fig. S1). The shapes of the three CB[n]-Pd NCs ( $n = 5, 7, 8$ ) are irregular and the small near spherical nanoparticles tend to gather together, thereby decreasing the exposed surface area. The catalytic performances for these three Pd NCs are tested by model reaction. The desired product was obtained in 30%, 66%, and 65% yields for CB[5]-, CB[7]-, and CB[8]-Pd NCs, respectively (Table 1, entries 25, 26, and 27). Such distinct catalytic performance of the CB[n]-Pd NCs may be explained by the structure symmetry, cavity, and volume size on different CB[n]s, which leads to strong or weak interactions with the substrates. Generally, CB[n]s have superior molecular recognition properties to form inclusion complexes

through hydrophobic binding or ion–dipole interactions with other molecules, especially for CB[7] and CB[8] with relatively larger cavities [34,35]. Herein,  $^1\text{H}$  NMR spectra were adopted to verify the interaction between CB[n]s and substrates. As the stacked  $^1\text{H}$  NMR spectra shown in Figs. S2 and S3, there is no obvious NMR peak shift for CB[6] after the addition of various substrates, suggesting no strong interaction between CB[6] and the substrates. Maybe the interaction between CB[6] and aryl halides substrates is too weak to form stable inclusion complexes. It is suggested that CB[6] only serves as a stabilizer for Pd NCs and does not participate the reaction. However, in the case of CB[5], CB[7], and CB[8], there are evident peak shifts and broadened peak width in NMR spectra (Fig. S2), indicating that CB[n]s ( $n = 5, 7, 8$ ) have a stronger interaction with the substrate than that of CB[6] does. Specifically for CB[8], the  $^1\text{H}$  NMR spectra reveal encapsulation-induced upfield chemical shifts for the aromatic resonances of substrate, which are consistent with inclusion in the shielding hydrophobic cavity.

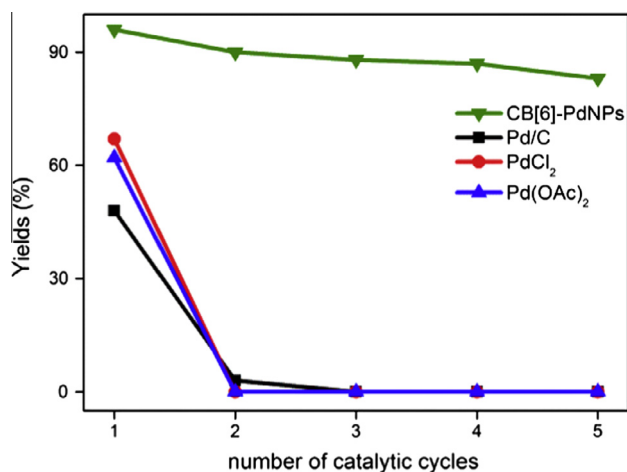


**Fig. 1.** (a) Recycling of the as-prepared Pd NCs, Pd/C, PdCl<sub>2</sub>, and Pd(OAc)<sub>2</sub> for direct arylation of pentafluorobenzene with bromobenzene.

The strong interaction of CB[*n*] (*n* = 5, 7, 8) with substrate might hinder the full interaction between substrate and Pd NCs, resulting in a lower catalytic performance for CB[*n*]-Pd NCs (*n* = 5, 7, 8) compared to CB[6]-Pd NPs. Such phenomenon also has been reported in the case of aromatic ring hydrogenation reactions by *RaMe*-cyclodextrins supported Ru(0) NCs [36]. Therefore, as evidenced from the above data and analysis, CB[6], which features the most stable symmetric structure, moderate cavity size and suitable volume size among common stable CB[*n*] (*n* = 5–8), should be the most suitable nanocatalyst stabilizer for harsh reactive conditions such as C–H bond activation.

With the optimized reaction conditions established, the substrate scope of the direct arylation of fluoroarenes with various aryl halides was investigated, and the results are summarized in Table 2. As depicted in Table 2, this reaction catalyzed by the as-prepared Pd NCs exhibits broad scope with respect to both the aryl halide and the fluoroarenes components. Pentafluorobenzene can be directly arylated by both aryl bromides and aryl iodides. Both electron-rich and electron-deficient aryl halides are reactive (Entries 3b–d and 3e–h in Table 1, respectively). Functional groups are also tolerated including ester, carbonyl, cyano, and trifluoromethyl (Entries 3e–h, Table 2). Bromonaphthalene also gives good yield of 85% (Entry 3i, Table 2). Tetrafluoro- and trifluoroarenes are found to be efficient for the direct arylated reaction with bromobenzene as coupling partner. For example, 1,2,4,5-tetrafluorobenzene and 1,2,3,5-tetrafluorobenzene can be obtained in good yields of 66% and 75%, respectively (Entries 3j and 3l, Table 2). Both of these two tetrafluorobenzenes possess two potential reaction sites, but the monoarylation products are preferentially generated in the as-prepared Pd NCs-catalyzed system. Additionally, 1,3,5-trifluorobenzene as less acidic trifluorobenzene also affords monoarylated product preferentially in moderate yields (Entry 3m–o, Table 2).

The recyclability of the as-prepared Pd NCs catalyst was studied by using the direct arylation of 1a with 2a as a model reaction. The as-prepared CB[6]-Pd NCs catalyst showed good recyclability over multiple cycles. As illustrated in Fig. 1, a sample of the Pd NCs has been recycled five times without significant loss in catalytic activity. Both PdCl<sub>2</sub> and Pd(OAc)<sub>2</sub> could catalyze the model reaction, giving 67% and 62% yields, respectively. However, neither of the two Pd salts is recyclable for the model reaction, like most of other homogeneous catalysts (red curve with dot and blue curve with triangle in Fig. 1). The commercial Pd/C only obtained 48% yield for the first run, which significantly underperformed the as-prepared Pd NCs catalyst. It is supposed that the commercial Pd/C

NCs have been sinter into large ones (TEM image in Fig. S4), leading to the catalytic activity decreased dramatically to 3% for the second run (black curve with square in Fig. 1). It is well known that the stabilization of the nanocatalyst against agglomeration during the catalytic procedure is of special importance, since the aggregation results in complete loss of catalytic activity. The as-prepared CB[6]-Pd NCs still preserve nearly 90% of its original reactivity for the fifth cycle, indicating that the CB[6] protected Pd NCs catalyst is highly stable and recyclable under the harsh reaction conditions. Such excellent activity and good recyclability successfully overcome the reusable problem for Pd salt as homogeneous catalyst and the loss of catalytic activity problem for commercial Pd/C caused by agglomeration during the catalytic reaction. Simultaneously, the good catalytic performance of the reusable Pd NCs catalyst greatly decreases the overall cost and improves the efficiency of the synthetic process for practical application.

### 3.3. Catalytically active species

To identify the catalytically active species from the as-prepared Pd NCs catalyzed system, Hg-poisoning and hot-filtration experiment test were carried out. A model reaction was added a drop of Hg(0) after 8 h and then heated more 16 h. No more products were detected during the subsequent process with Hg(0) added (Fig. S5). The result indicates that the amalgamation is formed on the surface of the Pd NCs, resulting in catalyst poisoning and the reaction ceasing. This suggests that the nature of catalytically active species is Pd(0) in this work [37–39]. Hot-filtration experiment was carried out for two hours for the model reaction to remove all solid materials. The filtrate was further reacted and monitored after fresh base and additive added. The filtrate gave no products during the additional reaction time, suggesting that all active catalytic species were removed by hot filtration. Such results suggest that the catalytic process may occur on the surface of Pd NCs, i.e., the direct arylation catalyzed by the as-prepared Pd NCs is heterogeneous reaction pathways.

### 3.4. Characterization of the catalyst

In order to address the structural features of the as-prepared Pd NCs catalyst during the catalytic reaction, TEM and HR-TEM images of the Pd NCs before and after catalysis have been studied (Fig. 2c–f). Typical TEM image of the as-synthesized Pd NCs is shown in Fig. 2a, along with the obtained size-distribution histogram ( $3.8 \pm 0.3$  nm), which is homogeneously dispersed. HR-TEM image of an individual nanoparticle shows clear lattice fringes with an interplanar distance of approximately 0.23 nm, corresponding to Pd(111) planes (Fig. 2b). There are clearly many structural defects on the surface of the as-prepared Pd NCs, indicated by the corresponding fast Fourier transform (FFT) diffraction pattern of the HR-TEM image (Fig. 2b, insert). Numerous researches demonstrated experimentally and computationally that small NCs possess a high percentage of surface atoms. The smaller the NCs, the more abundant of step edges and corners or other defect sites are on the surface. Surface defects, featured coordinative unsaturation, have an excellent reactivity for the large adsorption energy to preferentially adsorb the substrates and the strong bonding ability with one or two atoms of the adsorbate, thereby enhancing the catalytic performance [40–42]. Hence, the uniform dispersed small Pd NCs catalyst exhibits unique excellent catalytic properties in this work. As shown in Fig. 2c, most of the Pd NCs after catalysis maintain the uniform dispersion without obviously agglomeration, but increase in size to about 10 nm caused by Ostwald ripening. The HR-TEM images clearly show the distinct twin planes and stacking faults, demonstrating that the defects on the surface of the Pd NCs are maintained after catalysis (Fig. 2d and f). This demonstrates



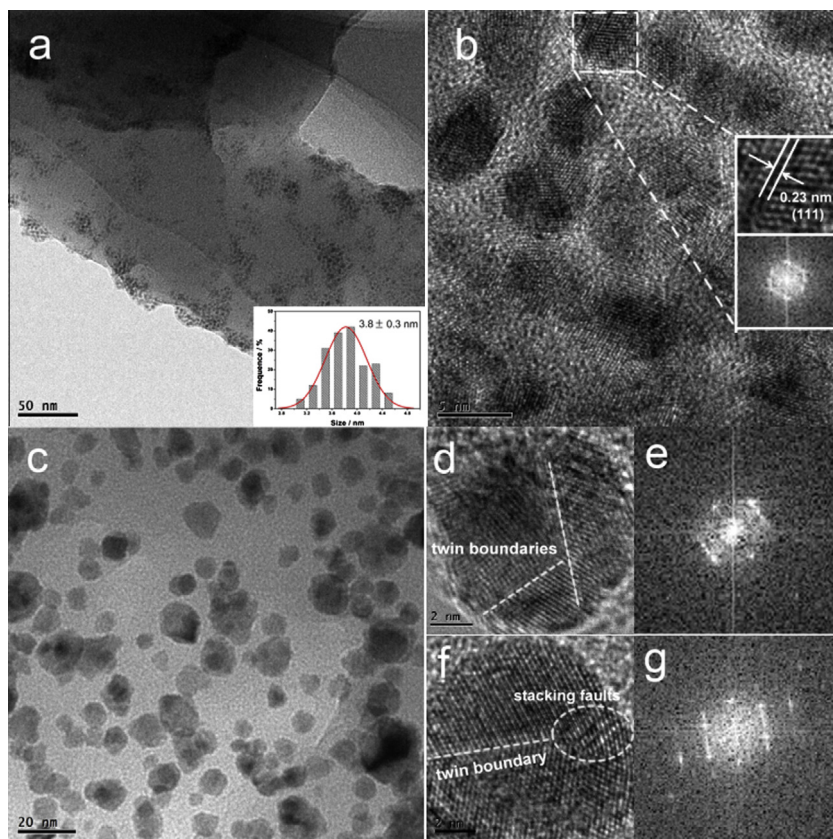


**Fig. 2.** TEM (a) and HR-TEM (b) images of the as-prepared Pd NCs before catalysis (insert is the corresponding FFT diffraction patterns of the square areas); TEM (c) and HR-TEM (d and f) images of the as-prepared Pd NCs after catalysis; and (e) and (g) are the corresponding FFT diffraction patterns of (d) and (f), respectively.

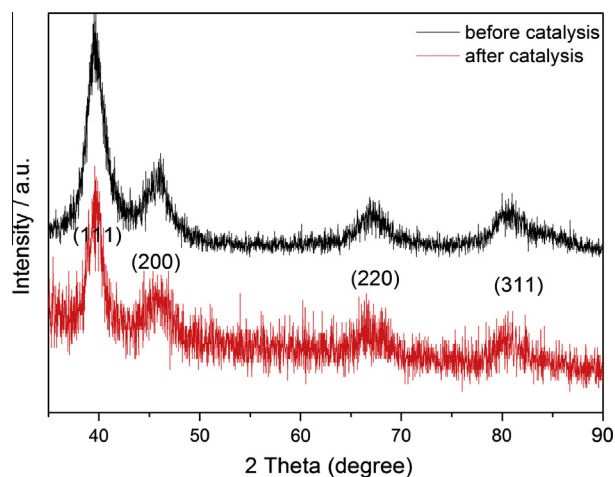


**Fig. 3.** XRD of CB[6]-Pd NCs before (black curve) and after catalysis (red curve). (For the interpretation of the references to color in this figure legend, the reader is referred to the web version of this article.)

that CB[6] plays a key role in stabilizing structural defects on the Pd NCs surface and thus endows the reused Pd NCs catalyst with maintained catalytic activity.

We further characterized the phase purity of the catalyst by means of powder X-ray diffraction (XRD) (Fig. 3). The reflection for the Pd NCs after catalysis is exactly the same as that of freshly prepared one, appearing at around 40°, 46°, 68°, and 82°, corresponding to (111), (200), (220), and (311) crystalline planes of the face-centered cubic (fcc) lattice (JCPDS NO. 46-1043). The

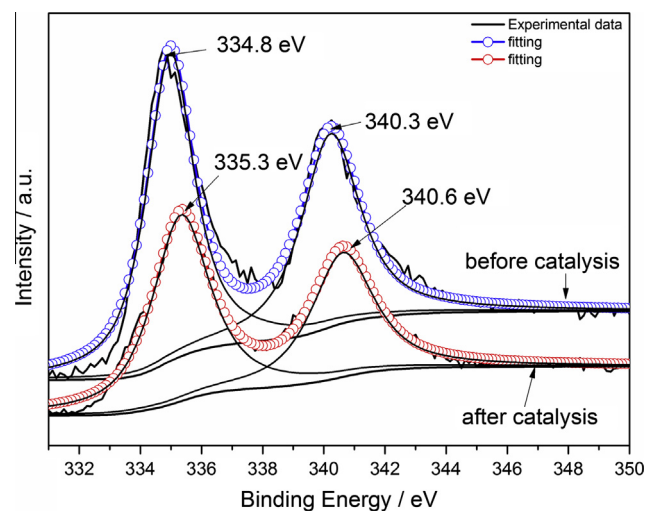


**Fig. 4.** XPS of CB[6]-Pd NPs before (blue curve) and after catalysis (red curve). (For the interpretation of the references to color in this figure legend, the reader is referred to the Web version of this article.)

surface chemistry of the CB[6]-Pd NCs catalyst was subjected to X-ray photoelectron spectroscopy (XPS) analysis to determine the oxidation state of Pd NCs. Fig. 4 displays XPS peak deconvolution results of Pd NCs catalyst before and after catalysis. The signals at 334.8 and 335.3 eV can be assigned to zero-valent Pd before and after catalysis, respectively [43]. No signal belongs to oxidized state Pd, indicating that the Pd NCs remain the zero-valent state after catalysis. Such results agree well with XRD results. The XPS

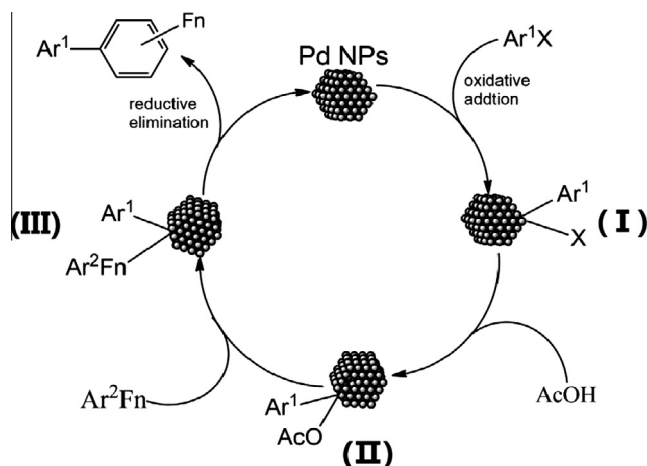


**Fig. 5.** Proposed catalytic cycles for the as-prepared Pd NPs catalyzed direct arylation of unactivated electron-efficient polyfluoroarene.

peak occurs a little shift to high binding energy after catalysis, which may be attributed to the variation on surface electron distribution after catalysis [44].

### 3.5. Presumable catalytic mechanism

According to the aforementioned results, we propose a plausible procedure for the catalysis. Fig. 5 illustrates that the catalytic reaction may undergo four successive processes. Presumably, the oxidative addition of aryl halides with Pd NPs forms the intermediate (I), then followed by an acid-mediated dehalogenation process giving intermediate (II). Subsequently, a ligand substitution process occurs in the presence of polyfluoroarene forming intermediate (III). Finally, a reductive elimination gives the desired coupling product.

## 4. Conclusions

In summary, we have developed a simple and general catalytic system for direct C–H functionalization of polyfluoroarene, by which a broad range of substrates can be employed with satisfactory yields of the product. The catalytic procedure is safe to air and moisture using the as-prepared Pd NPs as catalysts with significantly noble metal loading. And the Pd NPs can be effectively recycled multiple times without obvious loss of activity. Such a Pd NPs catalyst successfully overcomes the reusable problem of Pd salts in homogeneous catalysis as well as the loss of catalytic activity problem of commercial Pd/C caused by agglomeration during the catalytic procedure. Driven by all these advantages, the as-prepared Pd NPs catalysts will benefit its applications for economical processes in pharmaceutical industry and other benign chemical industries.

## Acknowledgment

We acknowledge financial support from the 973 Program (2011CB932504 and 2012CB821705), the NSFC (21221001, 21203199, and 21331006), the Fujian Key Laboratory of Nanomaterials (2006L2005), and the “Strategic Priority Research Program” of CAS (XDA09030102).

## Appendix A. Supplementary material

Supplementary data associated with this article can be found, in the online version, at <http://dx.doi.org/10.1016/j.jcat.2014.10.013>.

## References

- [1] M. Lafrance, C.N. Rowley, T.K. Woo, K. Fagnou, Catalytic intermolecular direct arylation of perfluorobenzenes, *J. Am. Chem. Soc.* 128 (2006) 8754–8756.
- [2] J.J. Mousseau, A.B. Charette, Direct functionalization processes: a journey from palladium to copper to iron to nickel to metal-free coupling reactions, *Acc. Chem. Res.* 46 (2013) 412–424.
- [3] L. Ackermann, R. Vicente, A.R. Kapdi, Transition-metal-catalyzed direct arylation of (hetero)arenes by C–H bond cleavage, *Angew. Chem. Int. Ed.* 48 (2009) 9792–9826.
- [4] D. Alberico, M.E. Scott, M. Lautens, Aryl–aryl bond formation by transition-metal-catalyzed direct arylation, *Chem. Rev.* 107 (2007) 174–238.
- [5] L.G. Mercier, M. Leclerc, Direct (Hetero) arylation: a new tool for polymer chemists, *Acc. Chem. Res.* (2013).
- [6] M. Miura, M. Nomura, Direct arylation via cleavage of activated and unactivated C–H bonds, in: N. Miyaura (Ed.), *Cross-Coupling Reactions*, Springer, Berlin Heidelberg, 2002, pp. 211–241.
- [7] W. Liu, F. Tian, X. Wang, H. Yu, Y. Bi, Simple alcohols promoted direct C–H arylation of unactivated arenes with aryl halides, *Chem. Commun.* 49 (2013) 2983–2985.
- [8] D.G. Yu, X. Wang, R.Y. Zhu, S. Luo, X.B. Zhang, B.Q. Wang, L. Wang, Z.J. Shi, Direct arylation/alkylation/magnesiation of benzyl alcohols in the presence of Grignard reagents via Ni-, Fe-, or Co-catalyzed sp<sup>3</sup> C–O bond activation, *J. Am. Chem. Soc.* 134 (2012) 14638–14641.
- [9] L.L. Chng, N. Erathodiyil, J.Y. Ying, Nanostructured catalysts for organic transformations, *Acc. Chem. Res.* 46 (2013) 1825–1837.
- [10] H. Miyamura, S. Kobayashi, Tandem oxidative processes catalyzed by polymer-incarcerated multimetallic nanoclusters with molecular oxygen, *Acc. Chem. Res.* 47 (2014) 1054–1066.
- [11] T. Yasukawa, H. Miyamura, S. Kobayashi, Polymer-incarcerated chiral Rh/Ag nanoparticles for asymmetric 1,4-addition reactions of arylboronic acids to enones: remarkable effects of bimetallic structure on activity and metal leaching, *J. Am. Chem. Soc.* 134 (2012) 16963–16966.
- [12] M. Sankar, N. Dimitratos, P.J. Miedziak, P.P. Wells, C.J. Kiely, G.J. Hutchings, Designing bimetallic catalysts for a green and sustainable future, *Chem. Soc. Rev.* 41 (2012) 8099–8139.
- [13] M.A. Mahmoud, R. Narayanan, M.A. El-Sayed, Enhancing colloidal metallic nanocatalysis: sharp edges and corners for solid nanoparticles and cage effect for hollow ones, *Acc. Chem. Res.* 46 (2013) 1795–1805.
- [14] R. Narayanan, M.A. El-Sayed, Effect of colloidal nanocatalysis on the metallic nanoparticle shape: the Suzuki reaction, *Langmuir* 21 (2005) 2027–2033.
- [15] R.V. Jagadeesh, A.E. Surkus, H. Junge, M.M. Pohl, J. Radnik, J. Rabeah, H. Huan, V. Schunemann, A. Bruckner, M. Beller, Nanoscale Fe<sub>2</sub>O<sub>3</sub>-based catalysts for selective hydrogenation of nitroarenes to anilines, *Science* 342 (2013) 1073–1076.
- [16] F.A. Westerhaus, R.V. Jagadeesh, G. Wienhofer, M.M. Pohl, J. Radnik, A.E. Surkus, J. Rabeah, K. Junge, H. Junge, M. Nielsen, A. Bruckner, M. Beller, Heterogenized cobalt oxide catalysts for nitroarene reduction by pyrolysis of molecularly defined complexes, *Nat. Chem.* 5 (2013) 537–543.
- [17] F. Shi, M.K. Tse, S. Zhou, M.M. Pohl, J. Radnik, S. Hubner, K. Jahnisch, A. Bruckner, M. Beller, Green and efficient synthesis of sulfonamides catalyzed by nano-Ru/Fe(3)O(4), *J. Am. Chem. Soc.* 131 (2009) 1775–1779.
- [18] S. Noel, B. Leger, A. Ponchel, K. Philippot, A. Denicourt-Nowicki, A. Roucoux, E. Monflier, Cyclodextrin-based systems for the stabilization of metallic (0) nanoparticles and their versatile applications in catalysis, *Catal. Today* 235 (2014) 20–32.
- [19] M.V. Rekharsky, Y. Inoue, Complexation thermodynamics of cyclodextrins, *Chem. Rev.* 98 (1998) 1875–1918.
- [20] F. Hapiot, A. Ponchel, S. Tilloy, E. Monflier, Cyclodextrins and their applications in aqueous-phase metal-catalyzed reactions, *C.R. Chim.* 14 (2011) 149–166.
- [21] M. Zhao, K. Deng, L. He, Y. Liu, G. Li, H. Zhao, Z. Tang, Core-shell palladium nanoparticle@metal-organic frameworks as multifunctional catalysts for cascade reactions, *J. Am. Chem. Soc.* 136 (2014) 1738–1741.
- [22] C.K. Tsung, J.N. Kuhn, W. Huang, C. Aliaga, L.I. Hung, G.A. Somorjai, P. Yang, Sub-10 nm platinum nanocrystals with size and shape control: catalytic study for ethylene and pyrrole hydrogenation, *J. Am. Chem. Soc.* 131 (2009) 5816–5822.
- [23] Y. Wu, D. Wang, P. Zhao, Z. Niu, Q. Peng, Y. Li, Monodispersed Pd–Ni nanoparticles: composition control synthesis and catalytic properties in the Miyaura–Suzuki reaction, *Inorg. Chem.* 50 (2011) 2046–2048.
- [24] Z. Niu, Q. Peng, Z. Zhuang, W. He, Y. Li, Evidence of an oxidative-addition-promoted Pd-leaching mechanism in the Suzuki reaction by using a Pd-nanostructure design, *Chem. Eur. J.* 18 (2012) 9813–9817.
- [25] M. Korzec, P. Bartczak, A. Niemczyk, J. Szade, M. Kapkowski, P. Zenderowska, K. Balin, J. Lelatkowski, J. Polanski, Bimetallic nano-Pd/PdO/Cu system as a highly effective catalyst for the Sonogashira reaction, *J. Catal.* 313 (2014) 1–8.
- [26] D.T. Tang, K.D. Collins, J.B. Ernst, F. Glorius, Pd/C as a catalyst for completely regioselective C–H functionalization of thiophenes under mild conditions, *Angew. Chem. Int. Ed.* 53 (2014) 1809–1813.
- [27] D.T. Tang, K.D. Collins, F. Glorius, Completely regioselective direct C–H functionalization of benzo[b]thiophenes using a simple heterogeneous catalyst, *J. Am. Chem. Soc.* 135 (2013) 7450–7453.
- [28] D. Bardelang, K.A. Udachin, D.M. Leek, J.A. Ripmeester, Highly symmetric columnar channels in metal-free cucurbit[n]uril hydrate crystals (n = 6, 8), *CrystEngComm* 9 (2007) 973–975.

- [29] M. Cao, J. Lin, H. Yang, R. Cao, Facile synthesis of palladium nanoparticles with high chemical activity using cucurbit[6]uril as protecting agent, *Chem. Commun.* 46 (2010) 5088–5090.
- [30] M. Cao, D. Wu, S. Gao, R. Cao, Platinum nanoparticles stabilized by cucurbit[6]uril with enhanced catalytic activity and excellent poisoning tolerance for methanol electrooxidation, *Chemistry* 18 (2012) 12978–12985.
- [31] T.C. Lee, O.A. Scherman, Formation of dynamic aggregates in water by cucurbit[5]uril capped with gold nanoparticles, *Chem. Commun. (Camb.)* 46 (2010) 2438–2440.
- [32] T.C. Lee, O.A. Scherman, A facile synthesis of dynamic supramolecular aggregates of cucurbit[n]uril ( $n = 5–8$ ) capped with gold nanoparticles in aqueous media, *Chemistry* 18 (2012) 1628–1633.
- [33] H. Zhang, M. Jin, Y. Xiong, B. Lim, Y. Xia, Shape-controlled synthesis of Pd nanocrystals and their catalytic applications, *Acc. Chem. Res.* 46 (2013) 1783–1794.
- [34] B.C. Pemberton, R. Raghunathan, S. Volla, J. Sivaguru, From containers to catalysts: supramolecular catalysis within cucurbiturils, *Chemistry* 18 (2012) 12178–12190.
- [35] J.W. Lee, S. Samal, N. Selvapalam, H.J. Kim, K. Kim, Cucurbituril homologues and derivatives: new opportunities in supramolecular chemistry, *Acc. Chem. Res.* 36 (2003) 621–630.
- [36] A. Denicourt-Nowicki, A. Roucoux, F. Wyrwalski, N. Kania, E. Monflier, A. Ponchel, Carbon-supported ruthenium nanoparticles stabilized by methylated cyclodextrins: a new family of heterogeneous catalysts for the gas-phase hydrogenation of arenes, *Chem. Eur. J.* 14 (2008) 8090–8093.
- [37] S.S. Soomro, F.L. Ansari, K. Chatziapostolou, K. Köhler, Palladium leaching dependent on reaction parameters in Suzuki-Miyaura coupling reactions catalyzed by palladium supported on alumina under mild reaction conditions, *J. Catal.* 273 (2010) 138–146.
- [38] K. Köhler, R.G. Heidenreich, S.S. Soomro, S.S. Pröckl, Supported palladium catalysts for Suzuki reactions: structure–property relationships, optimized reaction protocol and control of palladium leaching, *Adv. Synth. Catal.* 350 (2008) 2930–2936.
- [39] S.P. Andrews, A.F. Stepan, H. Tanaka, S.V. Ley, M.D. Smith, Heterogeneous or homogeneous? A case study involving palladium-containing perovskites in the Suzuki reaction, *Adv. Synth. Catal.* 347 (2005) 647–654.
- [40] C. Deraedt, D. Astruc, “Homeopathic” palladium nanoparticle catalysis of cross carbon–carbon coupling reactions, *Acc. Chem. Res.* 47 (2014) 494–503.
- [41] X. Guo, G. Fang, G. Li, H. Ma, H. Fan, L. Yu, C. Ma, X. Wu, D. Deng, M. Wei, D. Tan, R. Si, S. Zhang, J. Li, L. Sun, Z. Tang, X. Pan, X. Bao, Direct, nonoxidative conversion of methane to ethylene, aromatics, and hydrogen, *Science* 344 (2014) 616–619.
- [42] G.A. Somorjai, Modern surface science and surface technologies: an introduction, *Chem. Rev.* 96 (1996) 1223–1236.
- [43] M. Brun, A. Berthet, J.C. Bertolini, XPS, AES and Auger parameter of Pd and PdO, *J. Electron Spectrosc. Relat. Phenom.* 104 (1999) 55–60.
- [44] A. Gniewek, A.M. Trzeciak, J.J. Ziolkowski, L. Kepiński, J. Wrzyszczy, W. Tylus, Pd–PVP colloid as catalyst for Heck and carbonylation reactions: TEM and XPS studies, *J. Catal.* 229 (2005) 332–343.